British Geological Survey
NATURAL ENVIRONMENT RESEARCH COUNCIL

Mineralogical analysis of pan concentrates from Nigeria

Laboratory Operations Programme

Internal Report IR/09/040

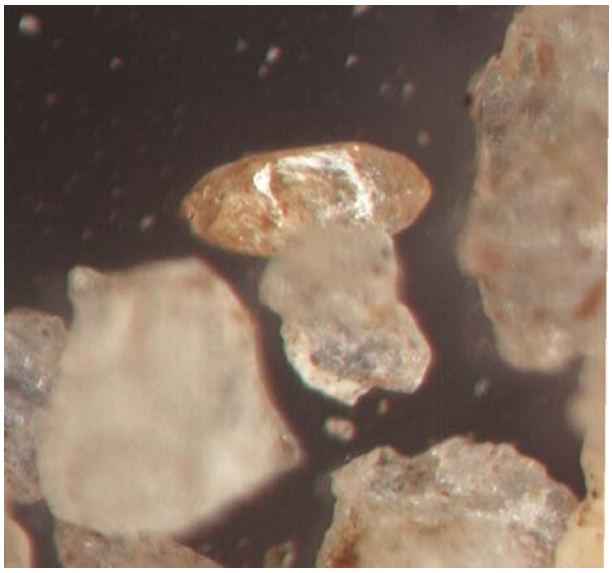

BRITISH GEOLOGICAL SURVEY

LABORATORY OPERATIONS PROGRAMME
INTERNAL REPORT IR/09/040

Mineralogical analysis of pan concentrates from Nigeria

S J Kemp, D Wagner, S Noble* and I Mounteney

*NERC Isotope Geosciences Laboratory

Keywords

X-ray diffraction, pan concentrates, zircon

Front cover

Zircon grain, sample MOS16

Bibliographical reference

KEMP, S J, WAGNER, D, NOBLE, S AND MOUNTENEY, I. 2009. Mineralogical analysis of pan concentrates from Nigeria. *British Geological Survey Internal Report*, IR/09/040. 21pp.

Keyworth, Nottingham British Geological Survey 2009

BRITISH GEOLOGICAL SURVEY

The full range of Survey publications is available from the BGS Sales Desks at Nottingham and Edinburgh; see contact details below or shop online at www.thebgs.co.uk

The London Information Office maintains a reference collection of BGS publications including maps for consultation.

The Survey publishes an annual catalogue of its maps and other publications; this catalogue is available from any of the BGS Sales Desks.

The British Geological Survey carries out the geological survey of Great Britain and Northern Ireland (the latter as an agency service for the government of Northern Ireland), and of the surrounding continental shelf, as well as its basic research projects. It also undertakes programmes of British technical aid in geology in developing countries as arranged by the Department for International Development and other agencies.

The British Geological Survey is a component body of the Natural Environment Research Council.

Keyworth, Nottingham NG12 5GG

☎ 0115-936 3241 Fax 0115-936 3488
e-mail: sales@bgs.ac.uk
www.bgs.ac.uk
Shop online at: www.thebgs.co.uk

Murchison House, West Mains Road, Edinburgh EH9 3LA

☎ 0131-667 1000 Fax 0131-668 2683
e-mail: scotsales@bgs.ac.uk

London Information Office at the Natural History Museum (Earth Galleries), Exhibition Road, South Kensington, London SW7 2DE

☎ 020-7589 4090 Fax 020-7584 8270
☎ 020-7942 5344/45 email: bgslondon@bgs.ac.uk

Forde House, Park Five Business Centre, Harrier Way, Sowton, Exeter, Devon EX2 7HU

☎ 01392-445271 Fax 01392-445371

Geological Survey of Northern Ireland, Colby House, Stranmillis Court, Belfast, BT9 5BF

☎ 028-9038 8462 Fax 028-9038 8461

Maclean Building, Crowmarsh Gifford, Wallingford, Oxfordshire OX10 8BB

☎ 01491-838800 Fax 01491-692345

Sophia House, 28 Cathedral Road, Cardiff, CF11 9LJ

☎ 029–2066 0147 Fax 029–2066 0159

Parent Body

Natural Environment Research Council, Polaris House, North Star Avenue, Swindon, Wiltshire SN2 1EU

☎ 01793-411500 Fax 01793-411501
www.nerc.ac.uk

Contents

TABLES

FIGURES

1 Introduction

This report presents the results of mineralogical characterisation of a small suite of seven pan concentrate samples from Nigeria. The samples were submitted for analysis by Drs Roger Key and John Ridgway (BGS) as part of the 'Technical Assistance Services for the Geochemical Mapping of Nigeria' project which aims to provide baseline geoscientific information for mineral exploration and environmental management through a study of the distribution of important metallic elements.

Particular interest was expressed in determining the hosts for the elevated levels of Zr in the concentrates. Full sample details, including Zr geochemical data from X-ray fluorescence spectroscopy (XRFS) are listed in Table 1.

Table 1. Summary of samples submitted

Incoming sample number	BGS MPL code	Longitude	Latitude	Site lithology	Catchment lithology	Zr from XRFS analysis
MOS2B 250	MPLN854	06,40.80	09,56.25	Biotite granite, locally feldspar-phyric	'Older Granite'	606.1 ppm
MOS4D 250	MPLN855	06,25.59	09,40.41	Granite and biotite schist fragments in stream	Birnin Gwari Schist and 'Older Granite'	190.9 ppm
MOS7C 250	MPLN856	07,10.05	10,04.05	Granite, partly migmatitic	Kushaka Schist	842.4 ppm
MOS15A 250	MPLN857	06,56.54	09,05.36	Granite gneiss	Migmatitic Gneiss Complex	1668.8 ppm
MOS16D 250	MPLN858	06,56.49	09,05.41	Augen gneiss	Migmatitic Gneiss Complex	3.0 wt%
MOS17A 250	MPLN859	06,57.06	09,06.32		Migmatitic Gneiss Complex	1.6 wt%
MOS20A 250	MPLP078	07,00.93	09,07.13	Migmatitic gneiss	Sheared Migmatitic Gneiss Complex	0.7 wt%

2 X-ray diffraction analysis

2.1 PREPARATION

In order to achieve a finer and uniform particle-size for powder XRD analysis, approximately 3 g portions of the tema-milled material were micronised under acetone for 10 minutes and then spray-dried following the method and apparatus described by Hillier (1999). The spray-dried material was then front-loaded into standard stainless steel sample holders.

2.2 ANALYSIS

Whole-rock XRD analysis was carried out using a PANalytical X'Pert Pro series diffractometer equipped with a cobalt-target tube, X'Celerator detector and operated at 45kV and 40mA. The micronised/spray-dried samples were scanned from 4.5-85°2θ at 2.76°2θ/minute. Diffraction

data were initially analysed using PANalytical X'Pert Highscore Plus version 2.2a software coupled to the latest version of the International Centre for Diffraction Data (ICDD) database.

2.3 QUANTIFICATION

Following identification of the mineral species present in the sample, mineral quantification was achieved using the Rietveld refinement technique (e.g. Snyder & Bish, 1989) using PANalytical Highscore Plus software. This method avoids the need to produce synthetic mixtures and involves the least squares fitting of measured to calculated XRD profiles using a crystal structure databank. Errors for the quoted mineral concentrations are typically ±2.5% for concentrations >60 wt%, ±5% for concentrations between 60 and 30 wt%, ±10% for concentrations between 30 and 10 wt%, ±20% for concentrations between 10 and 3 wt% and ±40% for concentrations <3 wt% (Hillier *et al.*, 2001). Where a phase was detected but its concentration was indicated to be below 0.5%, it is assigned a value of <0.5%, since the error associated with quantification at such low levels becomes too large.

3 Results and discussion

The quantitative results of powder XRD analyses are summarised in Table 2.

Table 2. Summary of quantitative powder XRD analyses

Incoming sample number	BGS MPL code	mineral (%)									
		quartz	albite	K-feldspar	augite	amphibole	pyrite	ilmenite	zircon	'mica'	'kaolin'
MOS2B 250	MPLN854	84.1	5.0	6.2	0.7	nd	<0.5	nd	nd	1.5	2.3
MOS4D 250	MPLN855	81.2	6.1	6.4	0.7	nd	<0.5	<0.5	nd	4.0	1.3
MOS7C 250	MPLN856	77.1	4.5	15.1	0.7	nd	<0.5	<0.5	<0.5	1.9	nd
MOS15A 250	MPLN857	66.9	16.0	13.5	1.2	1.7	<0.5	<0.5	<0.5	<0.5	nd
MOS16D 250	MPLN858	58.8	14.4	16.2	1.9	3.8	<0.5	0.7	3.9	<0.5	nd
MOS17A 250	MPLN859	67.1	10.7	13.1	1.7	4.4	<0.5	0.7	2.0	<0.5	nd
MOS20A 250	MPLP078	68.0	9.7	8.2	1.7	4.7	<0.5	6.1	1.2	<0.5	nd

XRD analysis indicates that the samples are predominantly composed of quartz with subordinate amounts of feldspar (plagioclase and K-feldspar), pyroxene (augite) and traces of 'mica' (undifferentiated mica species possibly including muscovite, biotite, illite and illite/smectite), pyrite ± further minor-trace amounts of zircon, amphibole, ilmenite and 'kaolin' (undifferentiated kaolin group minerals possibly including kaolinite, halloysite etc). Such a mineralogical assemblage is commensurate with observations made using an optical microscope. Selected heavy mineral grains are shown in the photomicrographs (Figures 1 and 2). Note that the zircons in Figure 1d show different morphologies. One of the zircons, indicated to the right of the field-of-view, is a composite grain typical of those found in some migmatites. It is composed of a rounded core with overgrowths which in turn are not facetted. The remaining zircons shown in Figure 1d are euhedral.

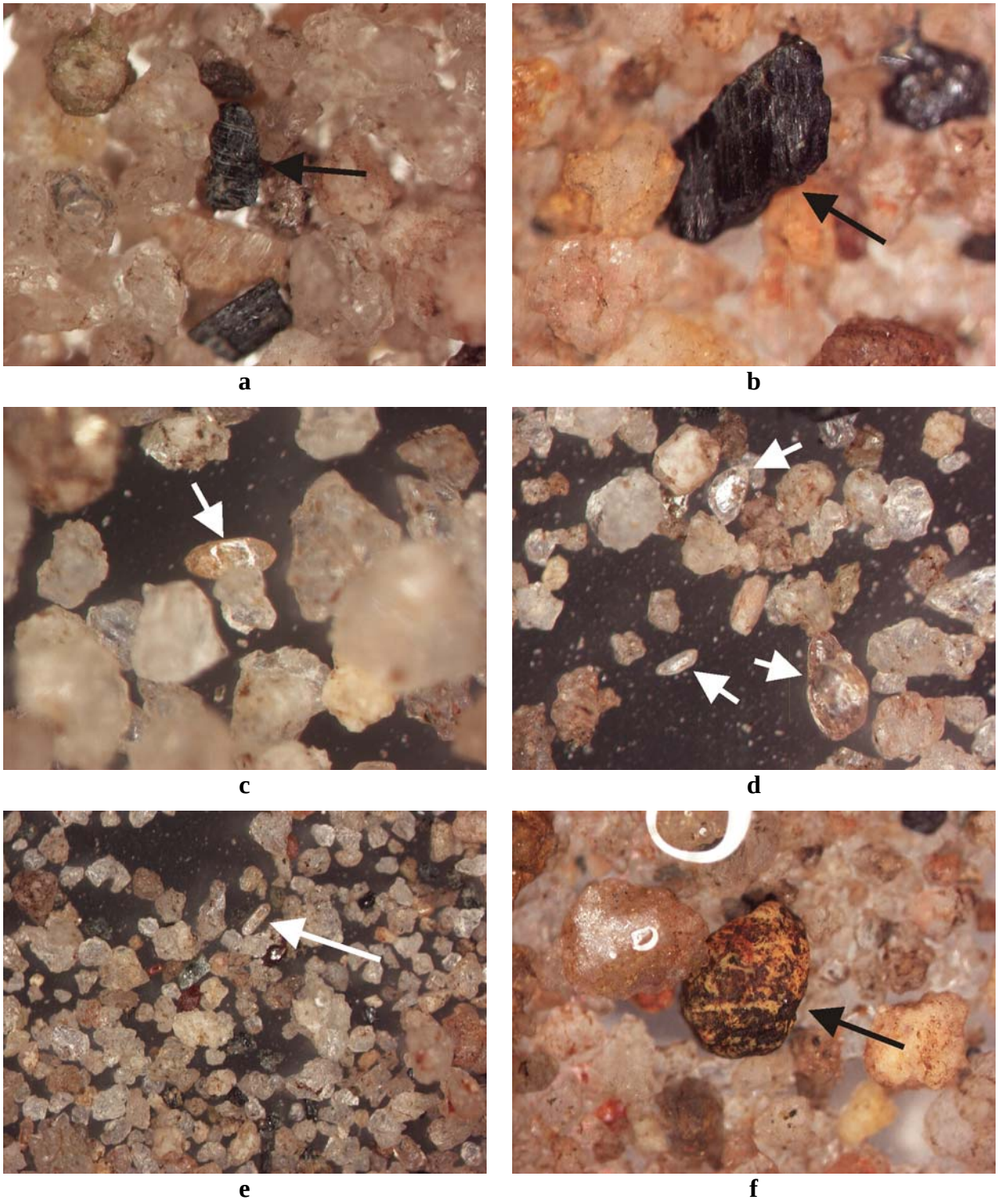

Figure 1. Optical photomicrographs of selected heavy mineral grains from the pan concentrates

a. Amphibole grain, sample MOS16
b. Amphibole grain, sample MOS20
c. Zircon grain, sample MOS16
d. Zircon grain, sample MOS16
e. Zircon grain, sample MOS16
f. ?Ilmenite grain, sample MOS20

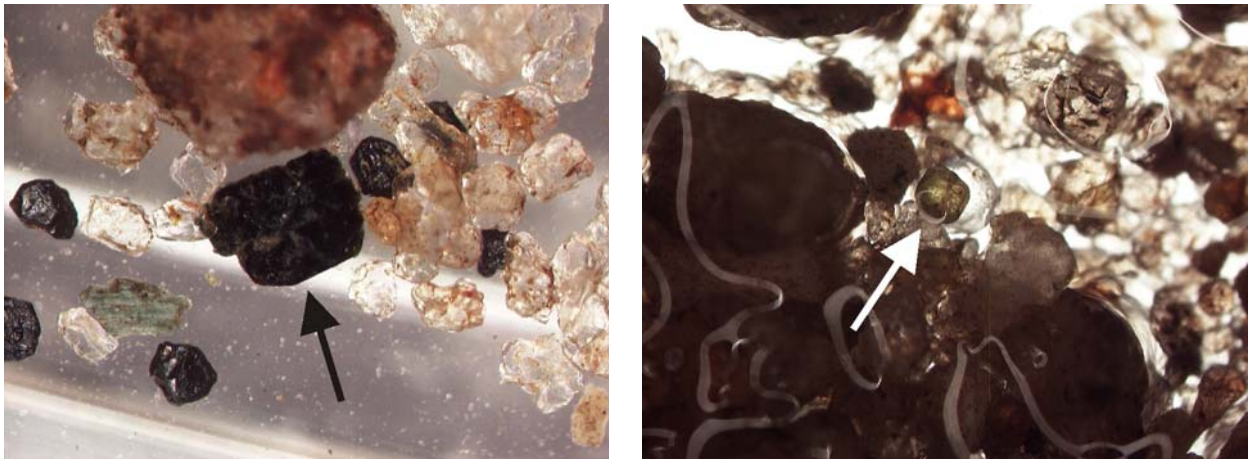

a **b**

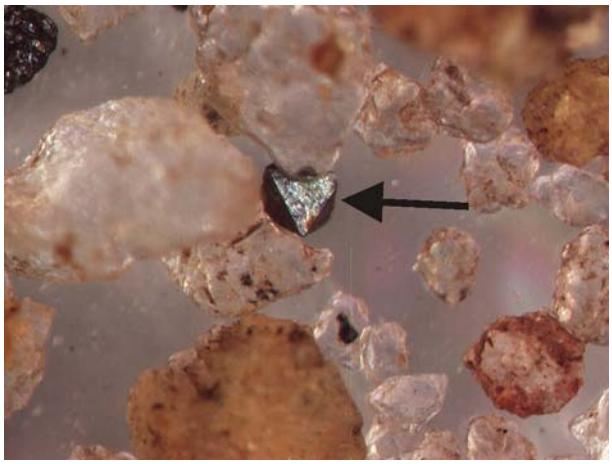

c

Figure 2. Optical photomicrographs of selected heavy mineral grains from the pan concentrates

a. Amphibole grain, sample MOS16 b. Monazite grain, sample MOS20
c. Uraninite/magnetite grain, sample MOS20

Cluster analysis of the powder diffraction data (Figure 3) indicates two relatively strong mineral assemblages:

- Group 1 samples (MOS2B, 4D and 7C) are characterised by relatively high quartz and phyllosilicate/clay mineral contents but relatively low feldspar, ferromagnesian mineral (pyroxene, amphibole) and zircon contents. These samples were sampled over granite and schist bedrock.
- Group 2 samples (MOS15A, 16D and 17A) are characterised by lower quartz, higher feldspar, very low phyllosilicate/clay mineral contents but relatively high ferromagnesian mineral and zircon contents. These samples were all sampled over migmatitic gneiss bedrock.
- Although apparently similar to the Group 2 samples, the non-clustered sample (MOS20A) shows an increased ilmenite concentration. MOS20A was also sampled over sheared migmatitic gneiss bedrock.

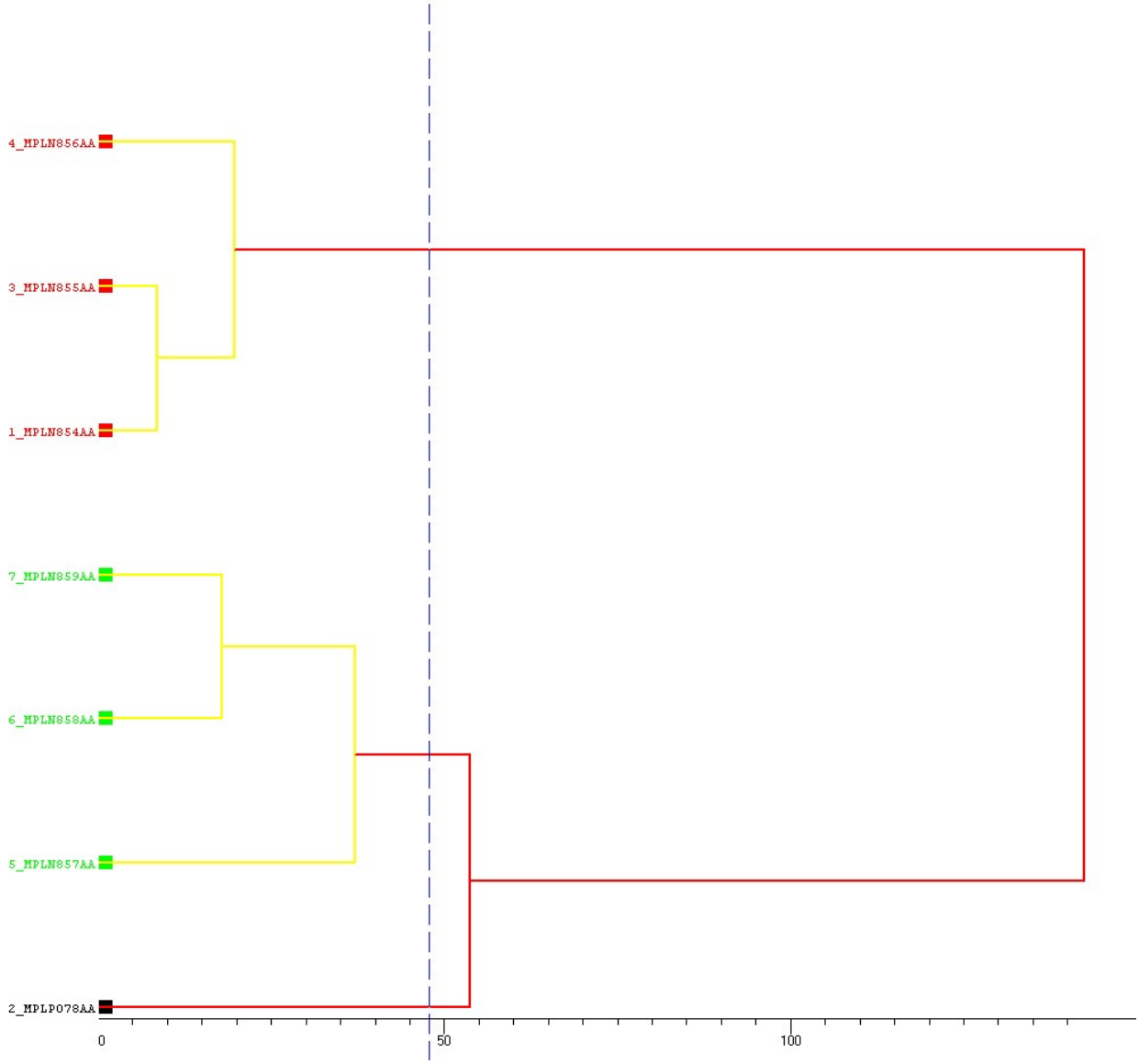

Figure 3. Cluster analysis dendrogram for the pan concentrate XRD traces

The only Zr-bearing phase identified by XRD in the pan concentrates was zircon ($ZrSiO_4$). XRD concentrations show an excellent correlation with XRFS geochemical data (Figure 4, $R^2 = 0.98$) with an apparent XRD detection limit of c.700 ppm Zr.

Zr concentrations derived from the XRD zircon contents confirm that zircon is the dominant host for Zr in the pan concentrates. The small, residual Zr concentrations may result from XRD quantification error or the presence of below XRD-detection levels of other Zr-bearing phases such as baddeleyite (ZrO2).

More accurate speciation of the heavy mineral fraction and potential identification of further Zr-bearing phases could be achieved if the quartz and feldspar component was removed using heavy media (e.g. Li-polytungstate) separation techniques prior to further XRD analysis.

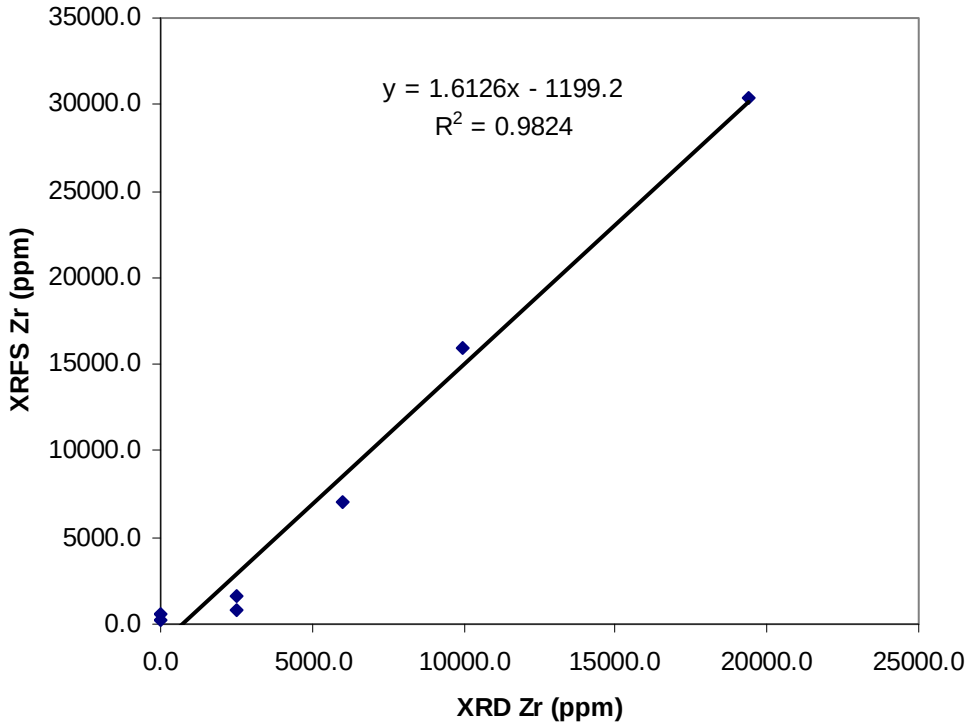

Figure 4. Correlation plot of XRD Zr (from zircon concentration) and XRFS Zr (both ppm)

4 Summary

- XRD analyses have been completed on a suite of seven pan concentrates from Nigeria.
- XRD analysis indicates similar assemblages to those observed from optical microscopy and which are predominantly composed of quartz with subordinate amounts of feldspar (plagioclase and K-feldspar), pyroxene (augite) and traces of 'mica', pyrite ± further minor-trace amounts of zircon, amphibole, ilmenite and 'kaolin'.
- Cluster analysis of XRD data indicates two relatively strong mineral assemblages with differing quartz, feldspar, phyllosilicate/clay mineral, ferromagnesian mineral and zircon contents. The mineral assemblage groupings correspond closely with the bedrock geology with samples collected from drainage basins underlain by migmatitic gneiss having different mineral assemblages from the other samples from schist and granitic terrains.
- The non-clustered sample (MOS20A) shows an increased ilmenite concentration.
- Zircon was the only Zr-bearing phase identified by XRD in the pan concentrates. Trace quantities of other Zr-bearing minerals (e.g. baddeleyite) may also be present but are below XRD detection limits.
- More accurate speciation of the heavy mineral fraction and potential identification of further Zr-bearing phases could be achieved if the quartz and feldspar component was removed using heavy media (e.g. Li-polytungstate) separation techniques prior to further XRD analysis.

References

Most of the references listed below are held in the Library of the British Geological Survey at Keyworth, Nottingham. Copies of the references may be purchased from the Library subject to the current copyright legislation.

HILLIER, S. 1999. Use of an air-brush to spray dry samples for X-ray powder diffraction. *Clay Minerals*, **34**, 127-135.

HILLIER, S., SUZUKI, K. AND COTTER-HOWELLS, J. 2001. Quantitative determination of Cerussite (lead carbonate) by X-ray powder diffraction and inferences for lead speciation and transport in stream sediments from a former lead mining area of Scotland. *Applied Geochemistry*, 16, 597-608.

SNYDER, R.L. AND BISH, D.L. 1989. Quantitative analysis. In: Bish, D.L., Post, J.E. (Eds), *Modern Powder Diffraction, Reviews in Mineralogy*, Volume 20, Mineralogical Society of America, USA, pp. 101-144 (Chapter 5).

Appendix: X-RAY DIFFRACTION TRACES:

KEY

The upper figure on each page shows the sample diffraction trace. The lower figure shows stick pattern data for the extracted sample peaks (orange) and the identified mineral standard data. Vertical axis – intensity (counts), horizontal axis - °2θ Co-Kα.

MOS2B 250

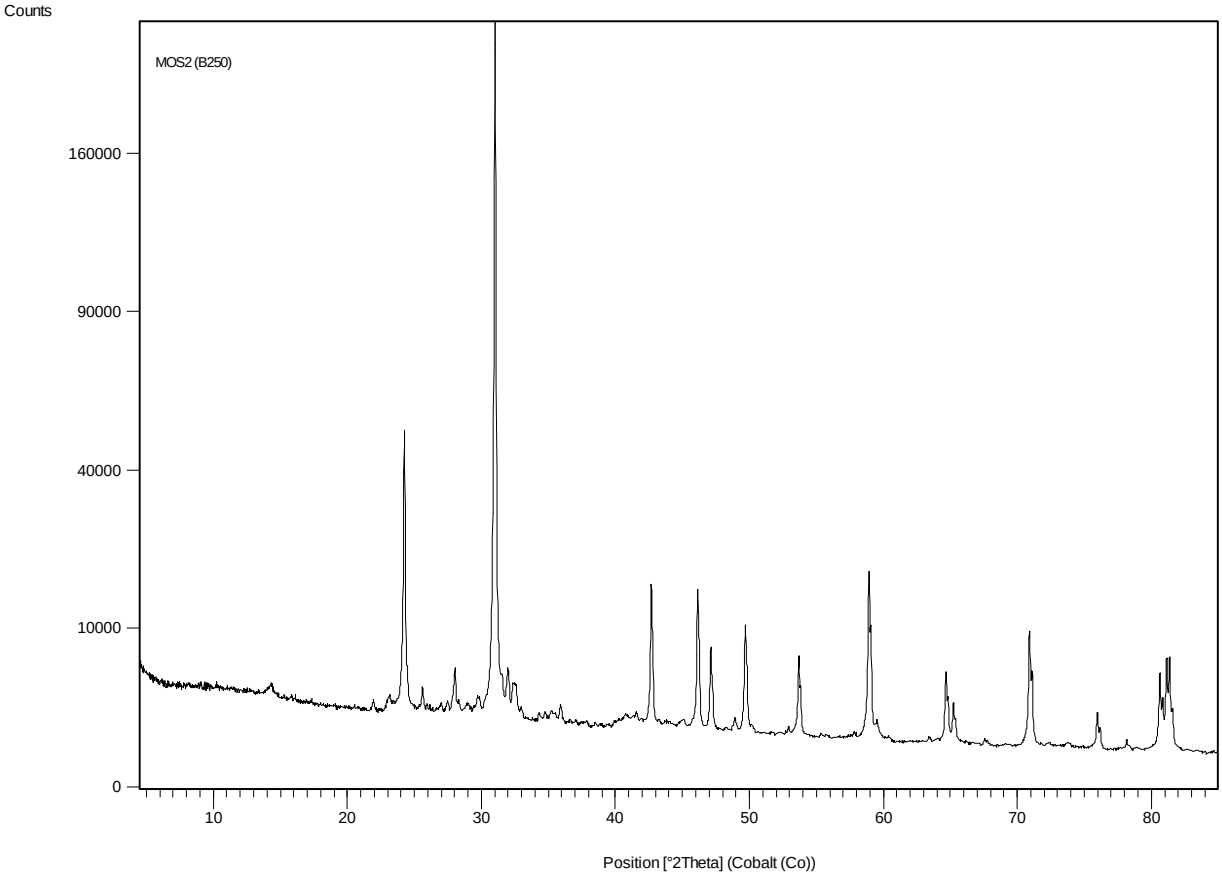
Counts
MOS2 (B250)
160000
90000
40000
10000
0
10
20
30
40
50
60
70
80
Position [°2Theta] (Cobalt (Co))

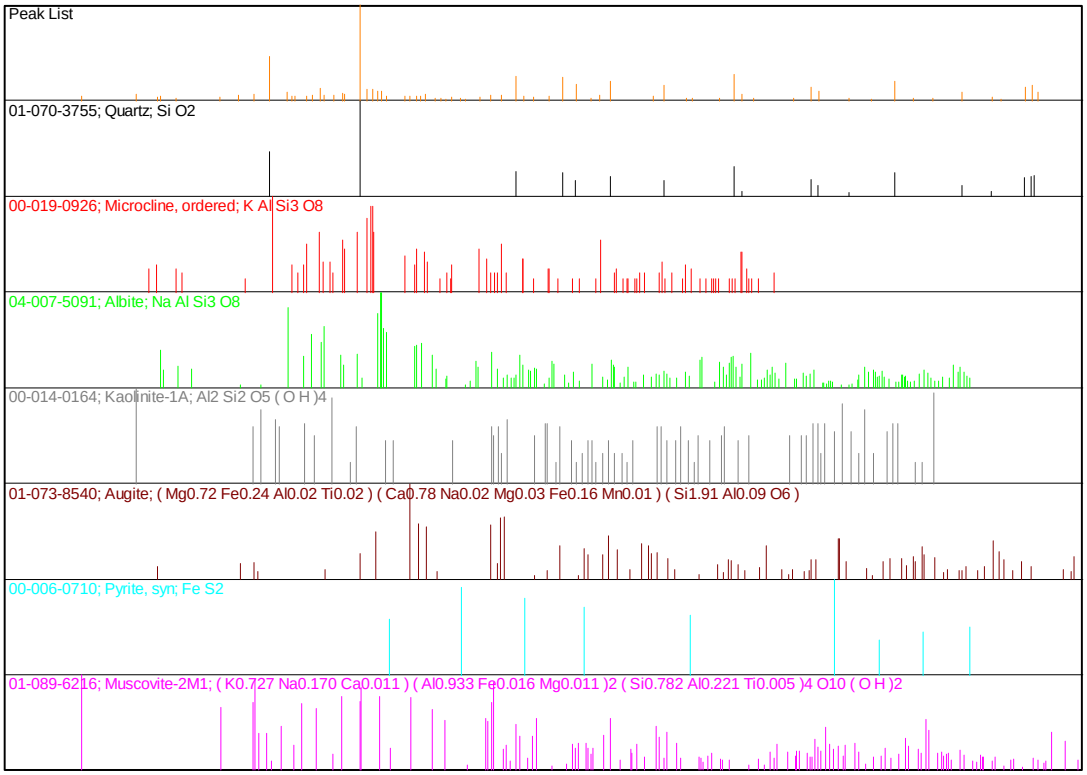
Peak List
01-070-3755; Quartz; Si O2
00-019-0926; Microcline, ordered; K Al Si3 O8
04-007-5091; Albite; Na Al Si3 O8
00-014-0164; Kaolinite-1A; Al2 Si2 O5 (O H)4
01-073-8540; Augite; (Mg0.72 Fe0.24 Al0.02 Ti0.02) (Ca0.78 Na0.02 Mg0.03 Fe0.16 Mn0.01) (Si1.91 Al0.09 O6)
00-006-0710; Pyrite, syn; Fe S2
01-089-6216; Muscovite-2M1; (K0.727 Na0.170 Ca0.011) (Al0.933 Fe0.016 Mg0.011)2 (Si0.782 Al0.221 Ti0.005)4 O10 (O H)2

MOS4D 250

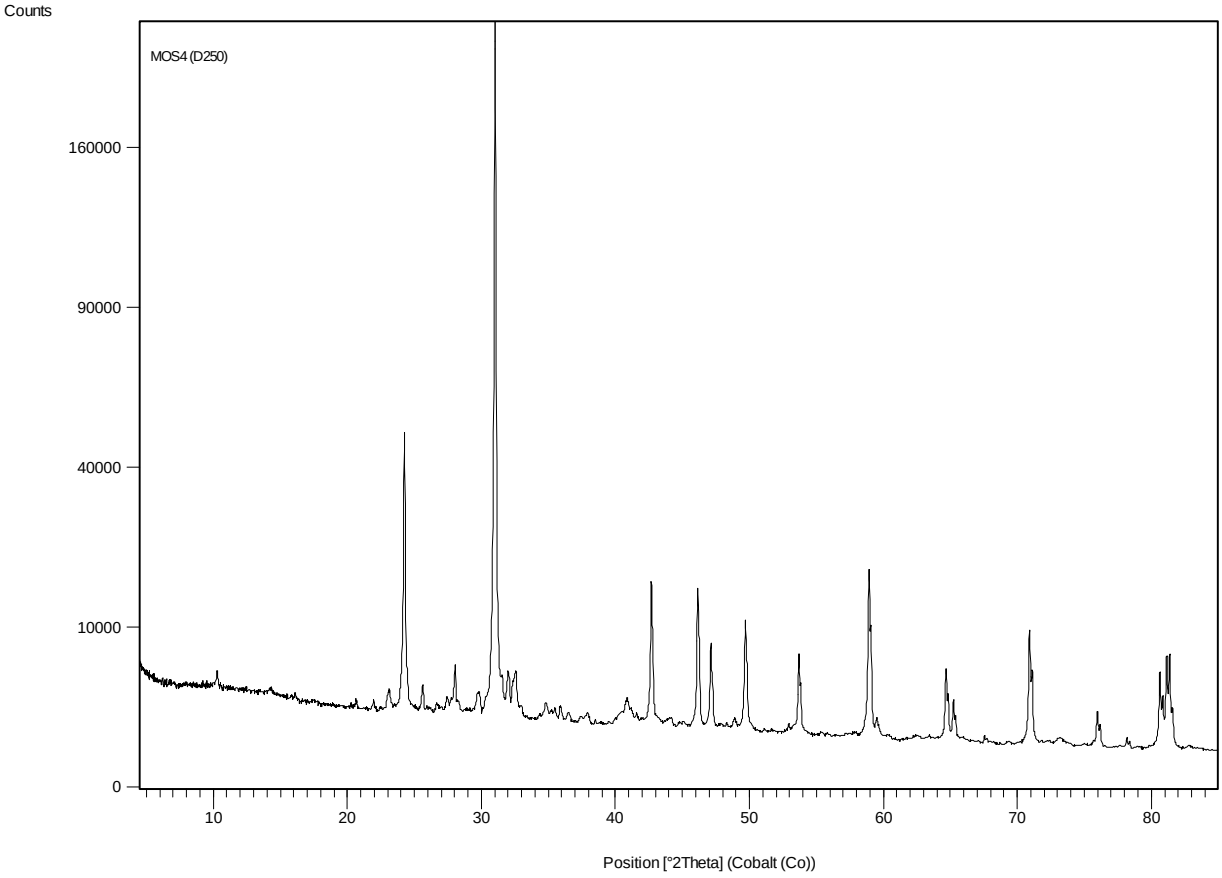
Counts
MOS4 (D250)
160000
90000
40000
10000
0
10
20
30
40
50
60
70
80
Position [°2Theta] (Cobalt (Co))

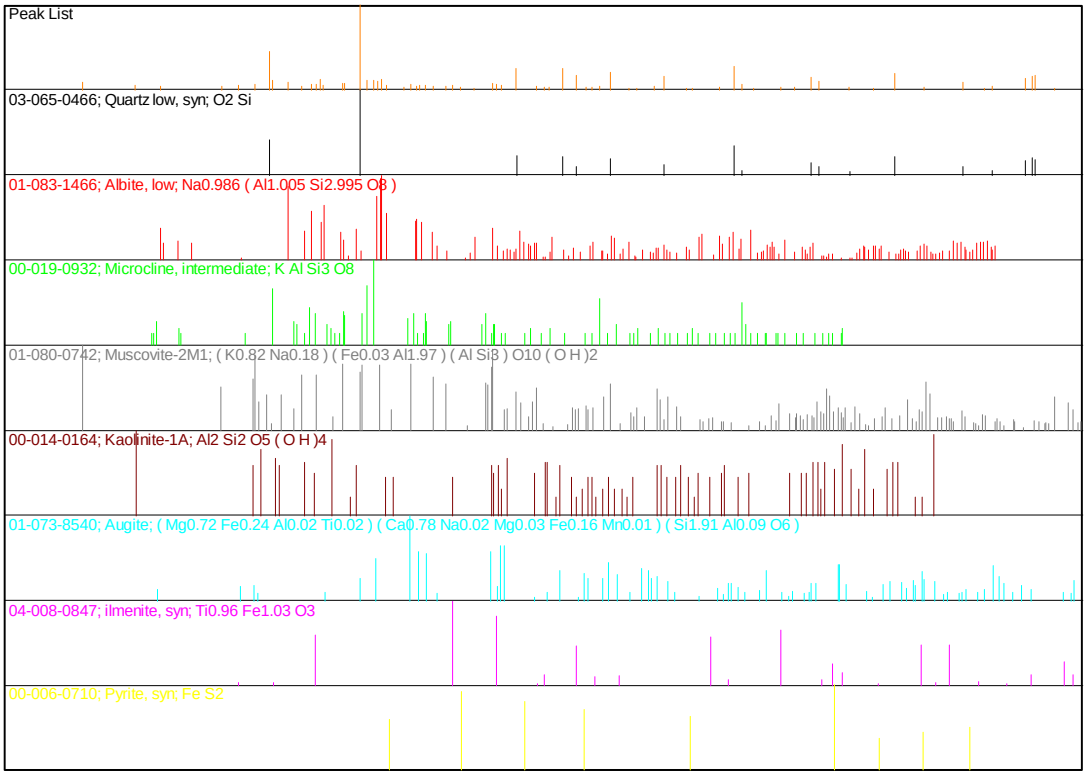
Peak List
03-065-0466; Quartz low, syn; O2 Si
01-083-1466; Albite, low; Na0.986 (Al1.005 Si2.995 O8)
00-019-0932; Microcline, intermediate; K Al Si3 O8
01-080-0742; Muscovite-2M1; (K0.82 Na0.18) (Fe0.03 Al1.97) (Al Si3) O10 (O H)2
00-014-0164; Kaolinite-1A; Al2 Si2 O5 (O H)4
01-073-8540; Augite; (Mg0.72 Fe0.24 Al0.02 Ti0.02) (Ca0.78 Na0.02 Mg0.03 Fe0.16 Mn0.01) (Si1.91 Al0.09 O6)
04-008-0847; ilmenite, syn; Ti0.96 Fe1.03 O3
00-006-0710; Pyrite, syn; Fe S2

MOS7C 250

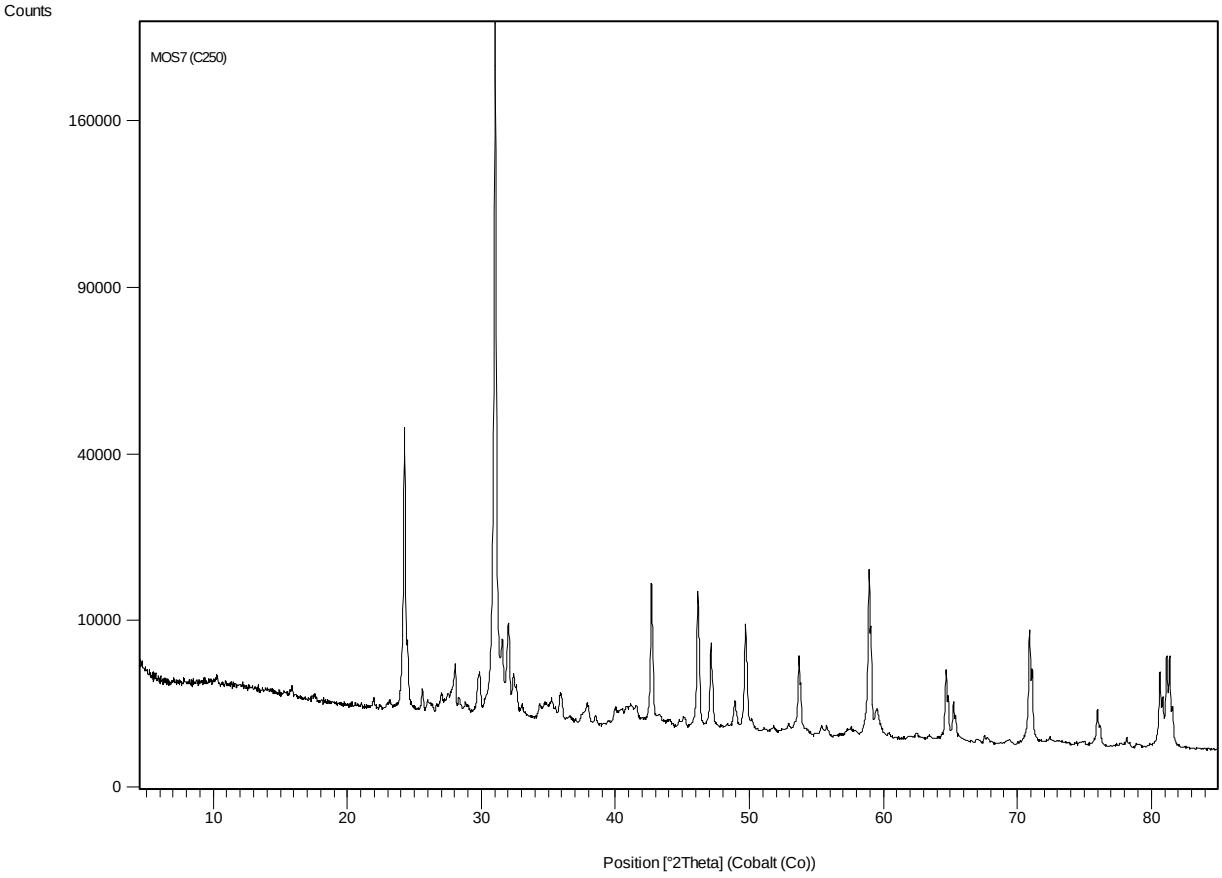
Counts
MOS7 (C250)
160000
90000
40000
10000
0
10
20
30
40
50
60
70
80
Position [°2Theta] (Cobalt (Co))

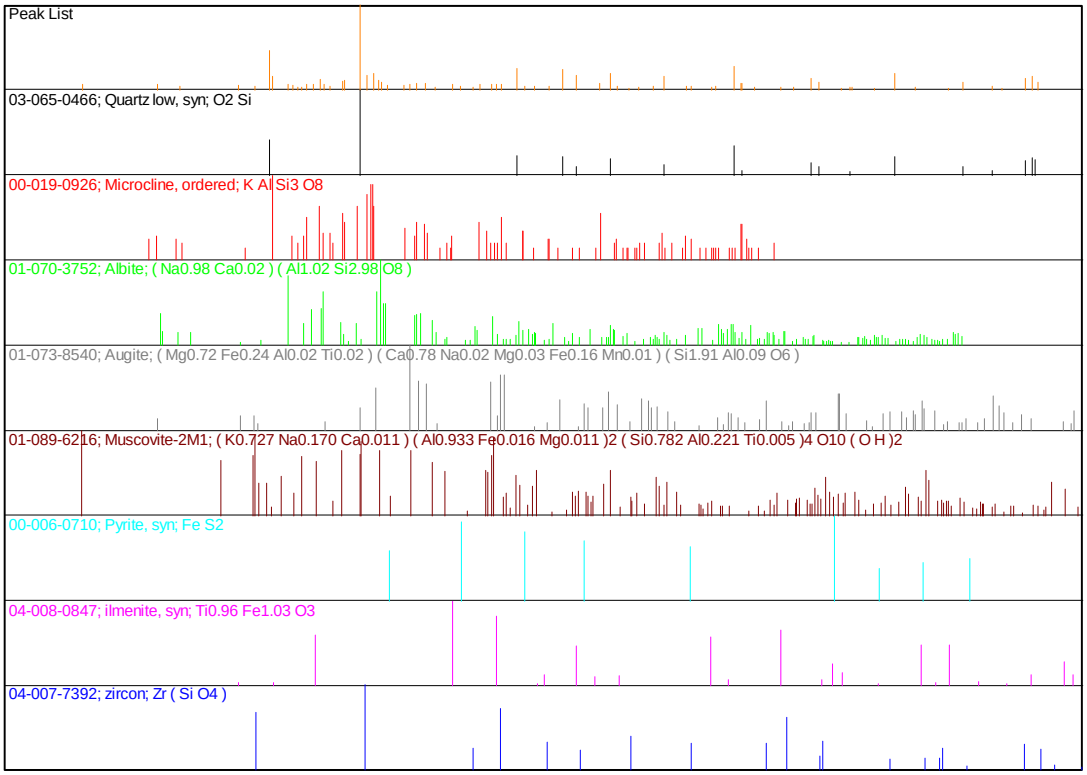
Peak List
03-065-0466; Quartz low, syn; O2 Si
00-019-0926; Microcline, ordered; K Al Si3 O8
01-070-3752; Albite; (Na0.98 Ca0.02) (Al1.02 Si2.98 O8)
01-073-8540; Augite; (Mg0.72 Fe0.24 Al0.02 Ti0.02) (Ca0.78 Na0.02 Mg0.03 Fe0.16 Mn0.01) (Si1.91 Al0.09 O6)
01-089-6216; Muscovite-2M1; (K0.727 Na0.170 Ca0.011) (Al0.933 Fe0.016 Mg0.011)2 (Si0.782 Al0.221 Ti0.005)4 O10 (O H)2
00-006-0710; Pyrite, syn; Fe S2
04-008-0847; ilmenite, syn; Ti0.96 Fe1.03 O3
04-007-7392; zircon; Zr (Si O4)

MOS15A 250

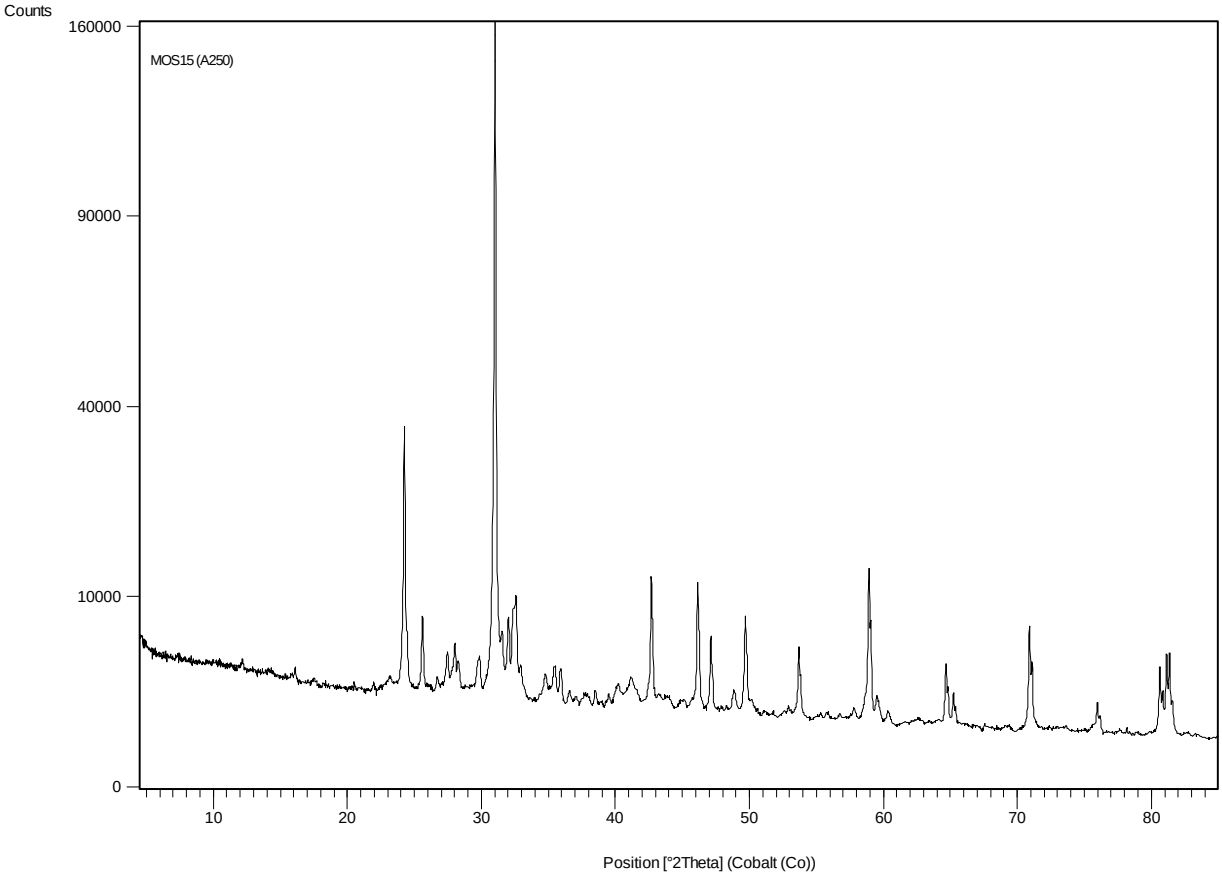
Counts
160000
90000
40000
10000
0
MOS15 (A250)
10
20
30
40
50
60
70
80
Position [°2Theta] (Cobalt (Co))

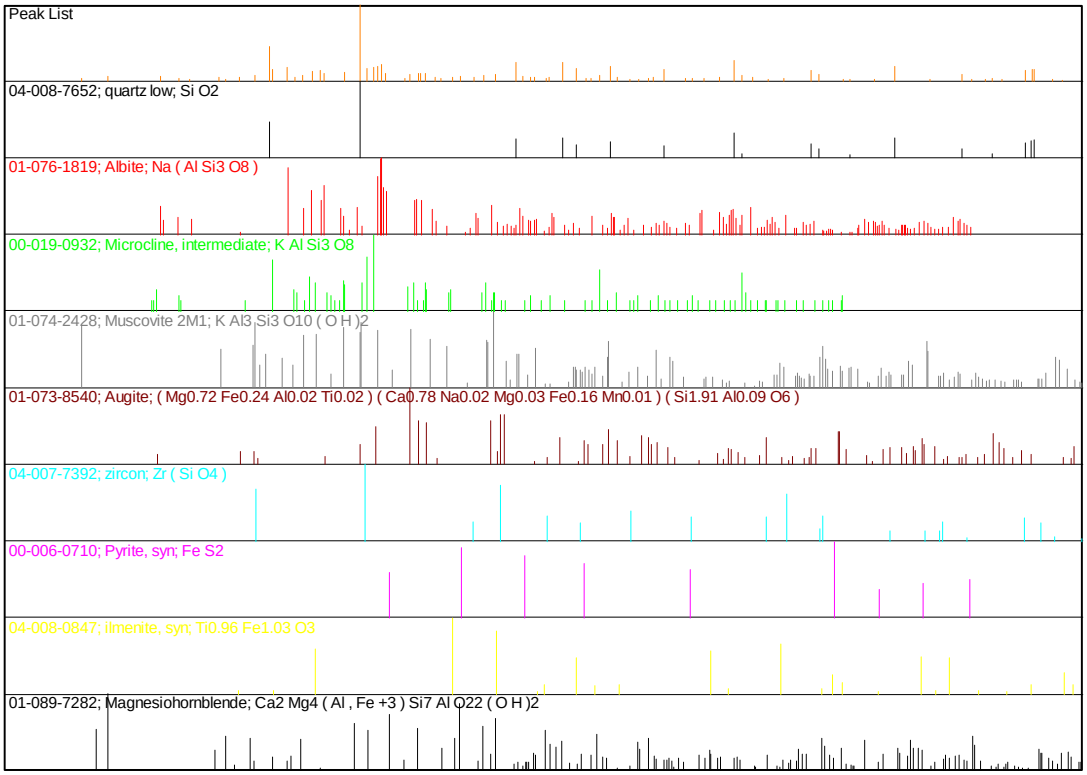
Peak List
04-008-7652; quartz low; Si O2
01-076-1819; Albite; Na (Al Si3 O8)
00-019-0932; Microcline, intermediate; K Al Si3 O8
01-074-2428; Muscovite 2M1; K Al3 Si3 O10 (O H)2
01-073-8540; Augite; (Mg0.72 Fe0.24 Al0.02 Ti0.02) (Ca0.78 Na0.02 Mg0.03 Fe0.16 Mn0.01) (Si1.91 Al0.09 O6)
04-007-7392; zircon; Zr (Si O4)
00-006-0710; Pyrite, syn; Fe S2
04-008-0847; ilmenite, syn; Ti0.96 Fe1.03 O3
01-089-7282; Magnesiohornblende; Ca2 Mg4 (Al , Fe +3) Si7 Al O22 (O H)2

MOS16D 250

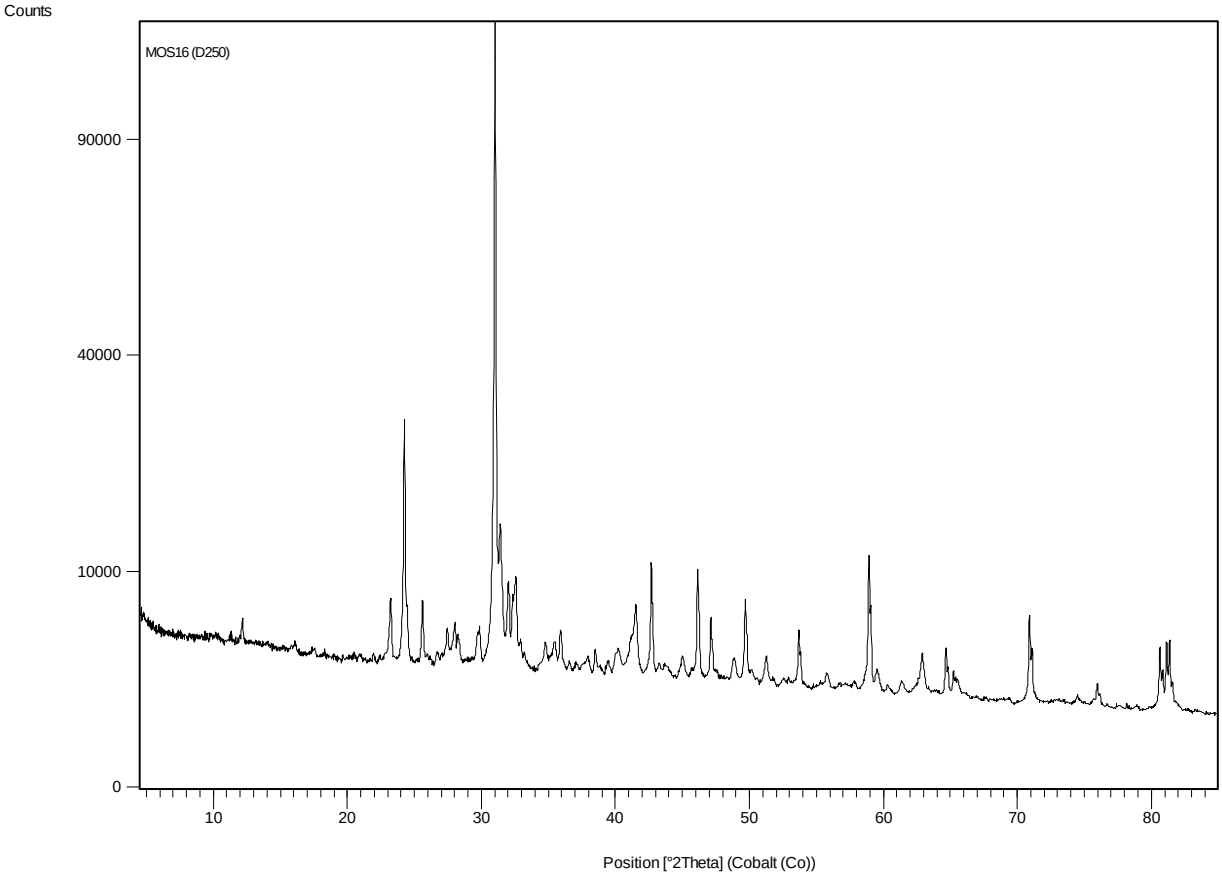
Counts
MOS16 (D250)
90000
40000
10000
0
10
20
30
40
50
60
70
80
Position [°2Theta] (Cobalt (Co))

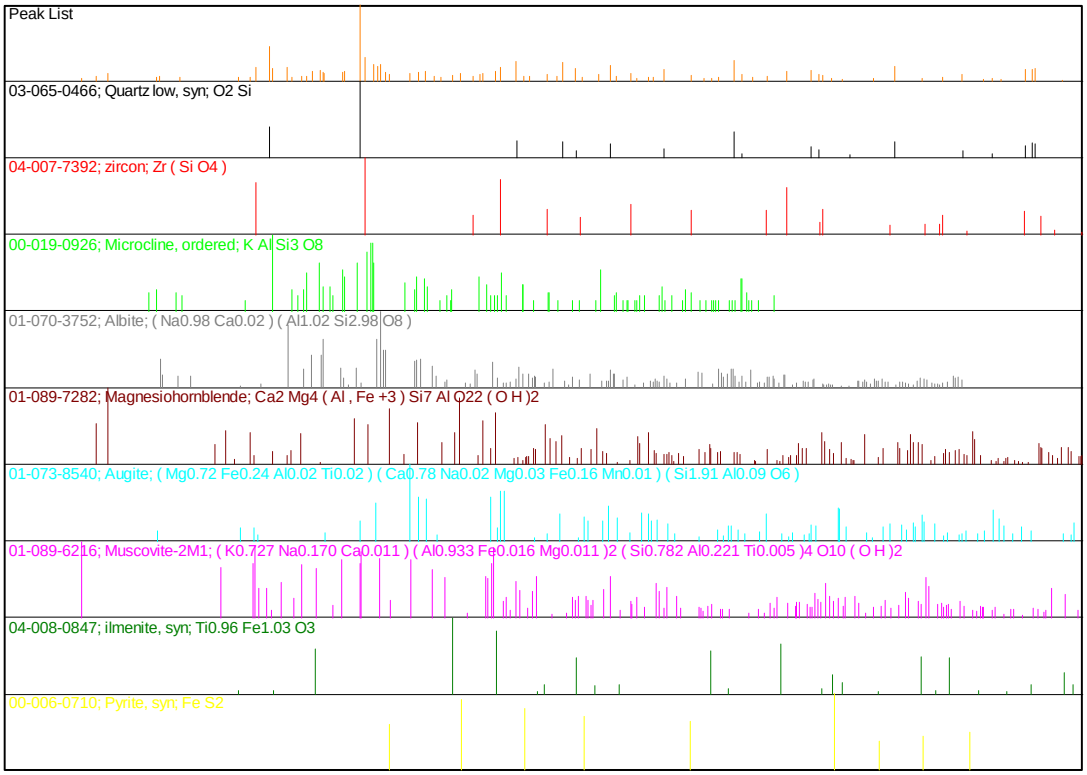
Peak List
03-065-0466; Quartz low, syn; O2 Si
04-007-7392; zircon; Zr (Si O4)
00-019-0926; Microcline, ordered; K Al Si3 O8
01-070-3752; Albite; (Na0.98 Ca0.02) (Al1.02 Si2.98 O8)
01-089-7282; Magnesiohornblende; Ca2 Mg4 (Al , Fe +3) Si7 Al O22 (O H)2
01-073-8540; Augite; (Mg0.72 Fe0.24 Al0.02 Ti0.02) (Ca0.78 Na0.02 Mg0.03 Fe0.16 Mn0.01) (Si1.91 Al0.09 O6)
01-089-6216; Muscovite-2M1; (K0.727 Na0.170 Ca0.011) (Al0.933 Fe0.016 Mg0.011)2 (Si0.782 Al0.221 Ti0.005)4 O10 (O H)2
04-008-0847; ilmenite, syn; Ti0.96 Fe1.03 O3
00-006-0710; Pyrite, syn; Fe S2

MOS17A 250

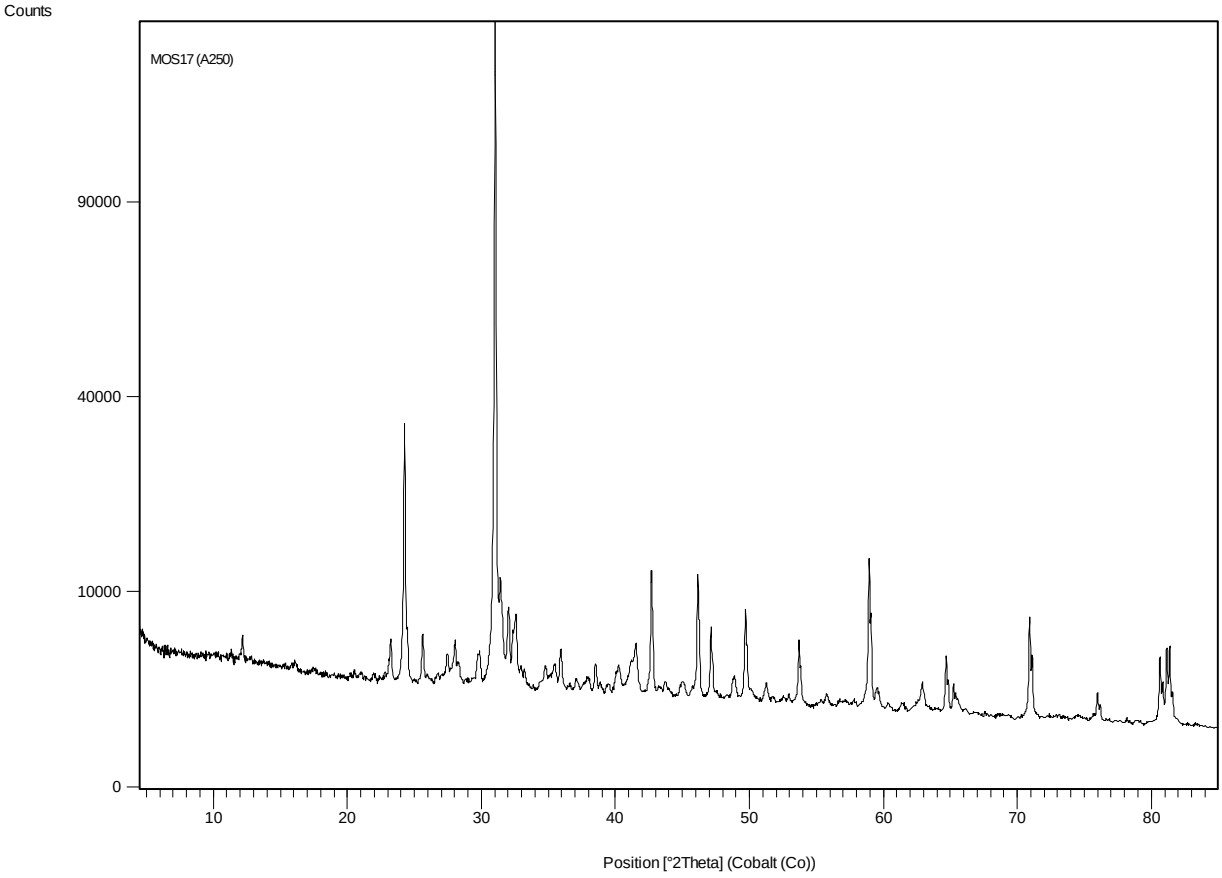
Counts
MOS17 (A250)
90000
40000
10000
0
10
20
30
40
50
60
70
80
Position [°2Theta] (Cobalt (Co))

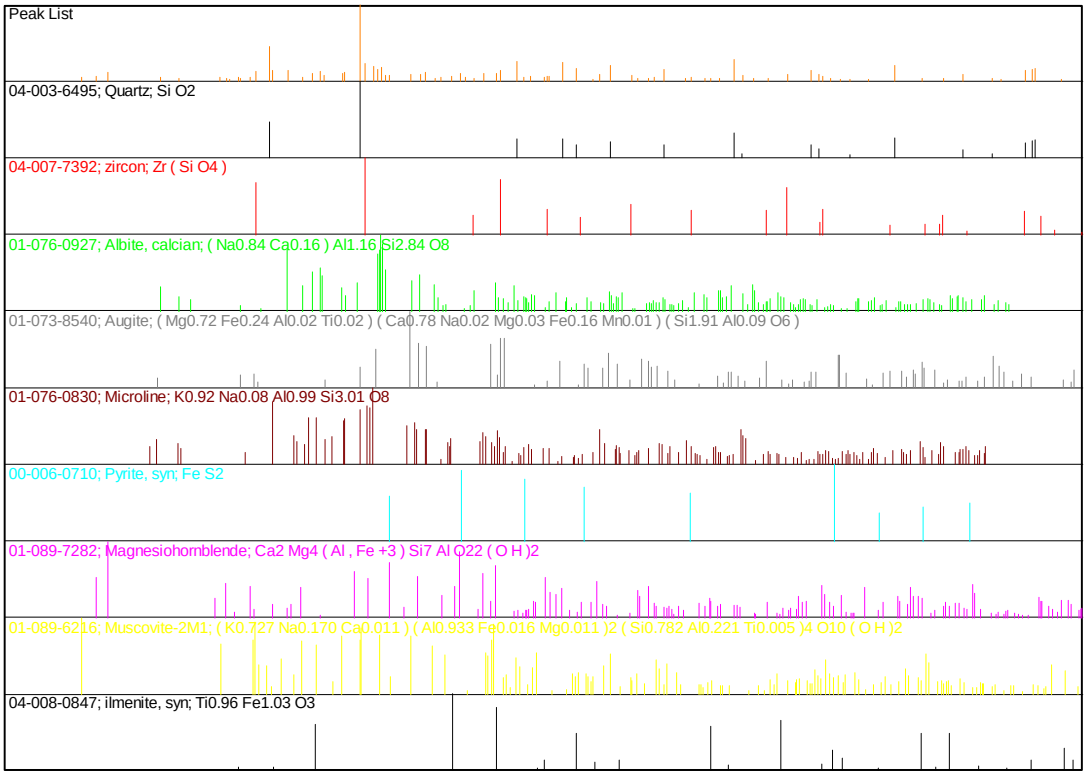
Peak List
04-003-6495; Quartz; Si O2
04-007-7392; zircon; Zr (Si O4)
01-076-0927; Albite, calcian; (Na0.84 Ca0.16) Al1.16 Si2.84 O8
01-073-8540; Augite; (Mg0.72 Fe0.24 Al0.02 Ti0.02) (Ca0.78 Na0.02 Mg0.03 Fe0.16 Mn0.01) (Si1.91 Al0.09 O6)
01-076-0830; Microline; K0.92 Na0.08 Al0.99 Si3.01 O8
00-006-0710; Pyrite, syn; Fe S2
01-089-7282; Magnesiohornblende; Ca2 Mg4 (Al , Fe +3) Si7 Al O22 (O H)2
01-089-6216; Muscovite-2M1; (K0.727 Na0.170 Ca0.011) (Al0.933 Fe0.016 Mg0.011)2 (Si0.782 Al0.221 Ti0.005)4 O10 (O H)2
04-008-0847; ilmenite, syn; Ti0.96 Fe1.03 O3

MOS20A 250

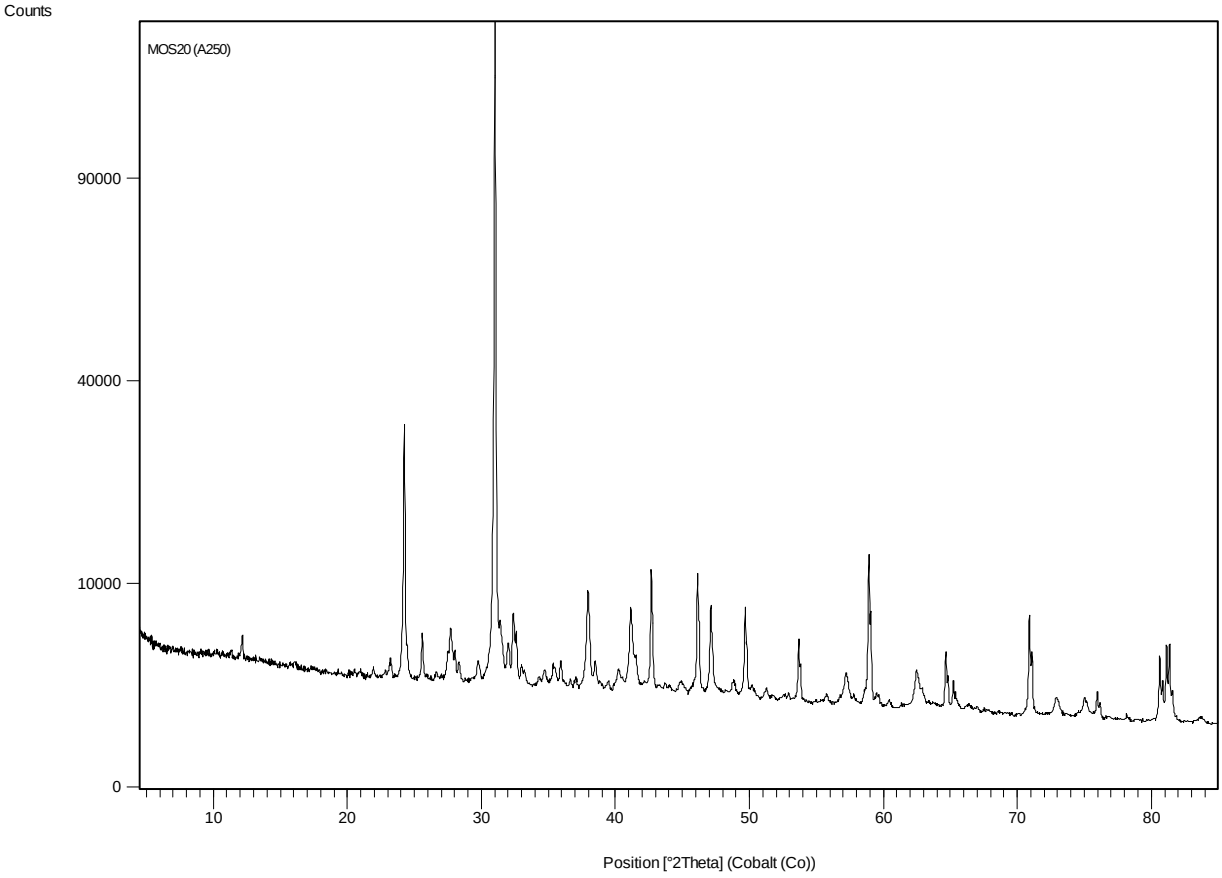
Counts
MOS20 (A250)
90000
40000
10000
0
10
20
30
40
50
60
70
80
Position [°2Theta] (Cobalt (Co))

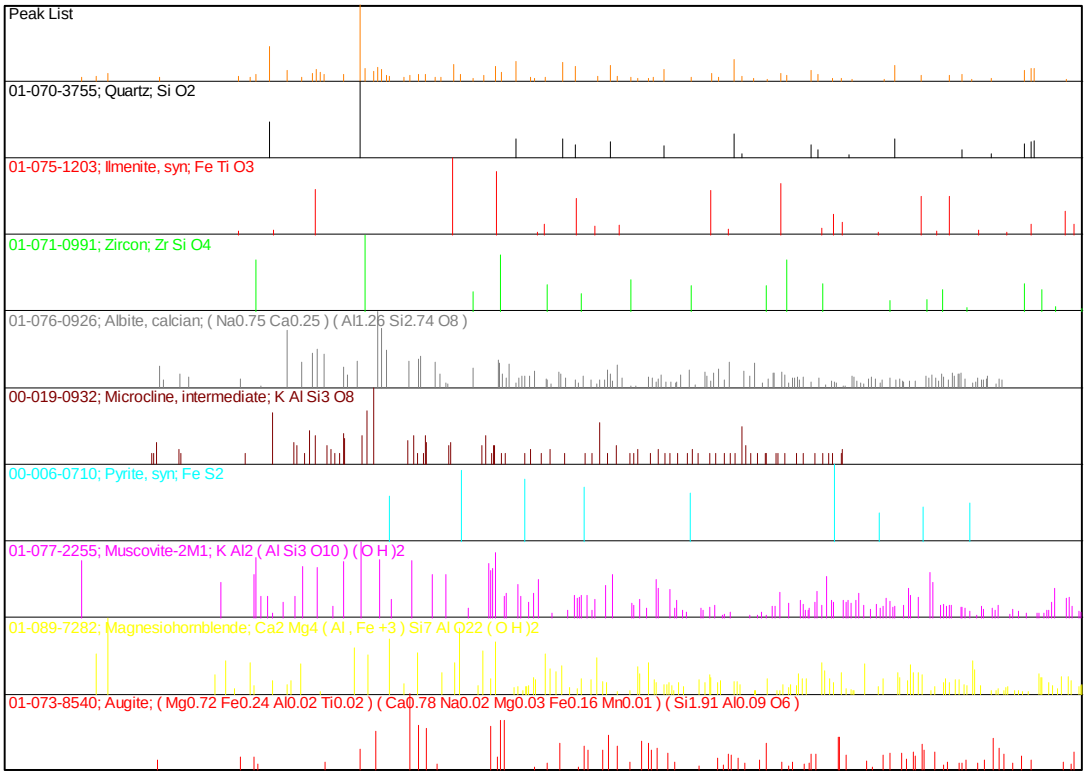
Peak List
01-070-3755; Quartz; Si O2
01-075-1203; Ilmenite, syn; Fe Ti O3
01-071-0991; Zircon; Zr Si O4
01-076-0926; Albite, calcian; (Na0.75 Ca0.25) (Al1.26 Si2.74 O8)
00-019-0932; Microcline, intermediate; K Al Si3 O8
00-006-0710; Pyrite, syn; Fe S2
01-077-2255; Muscovite-2M1; K Al2 (Al Si3 O10) (O H)2
01-089-7282; Magnesiohornblende; Ca2 Mg4 (Al , Fe +3) Si7 Al O22 (O H)2
01-073-8540; Augite; (Mg0.72 Fe0.24 Al0.02 Ti0.02) (Ca0.78 Na0.02 Mg0.03 Fe0.16 Mn0.01) (Si1.91 Al0.09 O6)